AN INTERFERENCE REFRACTOMETER FOR GASES AND LIQUIDS

W. Kinder

Heidenheim, Germany

Optik 24, 323-334 (1966/67)

Translated at CERN by B. Hodge
(Original: German)
Revised by H. MacCabe

(CERN Trans. Int. 73-4)

Geneva

February 1973

ABSTRACT

The paper deals with a differential refractometer for gas and liquid analyses which works on the principle of the Michelson interferometer. A description is given of the special optical design features as well as of the compensator. The instrument has a measuring accuracy of 1/100th wavelength and permits differences of refractive index in liquids to be determined to 1×10^{-7} and in gases to 1×10^{-8}. Measurements are made visually. However, mention is also made of a photoelectric system for automatic operation.

1. Historical Review and earlier Zeiss Equipment

Already at the beginning of the last century, interferometric methods were used for determining the refractive power of gases and liquids. On the basis of Young's interference experiment /1/ (a screen with two diffracting apertures), and its modification by A. Fresnel /2/ (double aperture), F. Arago /3/, with the assistance of Soleil and Duboscq, constructed the first known interference-refractometer.

The optical design of this equipment is shown in Figure 1. Arago had also at that time added a compensator (consisting of four glass plates). By rotating two compensator plates, it is possible to cancel the path difference produced by a substance inserted in the path of the rays; the angle of rotation is a measure of the refractive power of the substance inserted.[1] Shortly afterwards, M.J. Jamin built an interferometer /5/ based on the interference phenomenon of the so-called "Brewster's fringes" discovered by D. Brewster /4/. Figure 2 shows an early model of the Jamin interferometer, which was built by Carl Zeiss towards the end of the century. The Jamin compensator consists of two glass plates which are inclined towards each other at a fixed angle and are jointly rotated around a common axis. The picture does not show the chamber holding the substance under examination; this is inserted between the left interference plate and the compensator. The chamber, together with its temperature control equipment, can be seen in Figure 3; the latter shows a Jamin interferometer manufactured by Zeiss in about 1905 and used by F. Haber /8/ for his optical gas analysis experiments. In subsequent experiments, carried out by Haber in close collaboration with F. Löwe /10/ and the Zeiss works, another device was also tried out which operated on the Young-Fresnel-Arago principle. This type of device had already been used for the analysis of gases by Lord Rayleigh /7/ who had considerably improved it, particularly by introducing a cylindrical-

---

1. cf. G. Hansen /11/ and W. Nebe /18/ on the subject of compensators.

lens eyepiece and adding a fiducial beam path. Haber and Löwe /9/ realised that this type of interferometer offered a particularly high accuracy of measurement. They decided therefore to adopt this type of apparatus, which the Zeiss works started to manufacture in 1910. The equipment proved so satisfactory that it continued to be produced almost unchanged up to 1945. Improvements were incorporated which concerned the exterior design, the chambers and accessories, but not the measurement principle. A 1941 model, with a chamber for gases, is shown in Figure 4. Its optical design is set out in Figure 5. The laboratory interferometer, like the smaller portable interferometer, had many applications in the analysis of gases and liquids and was therefore widely used. A publication dating from 1926 gives already the addresses of more than 200 users of this interferometer. Among its very numerous applications we shall only mention a few: determination of the refractive index of gases and liquids; purity testing of gases; concentration measurements of gas and vapour mixtures; determination of the methane and CO_2 content of the air in mines; metabolism measurements; monitoring of the danger of explosion in tankers as a result of hydrocarbon vapours; and, finally, examination of drinking, river, lake and sea water /15/.

In spite of their many advantages, these interferometers had several serious shortcomings: the non-linearity of the compensator required; each apparatus to be individually calibrated with mercury light; taking outside readings on the drum was cumbersome; there were also shortcomings in temperature control which required special procedures for precision measurements /13/. The most troublesome factor was the lack of brightness, which is a source of difficulty when photoelectric adjustments and measurements are made. The lack of brightness was due not so much to insufficient illumination as to the principle of geometric beam splitting which requires a narrow slit in order to achieve the necessary angle of coherence. A system of multiple H slits could produce improvements, but an essential change cannot be achieved in this way. Hence, already in 1941, at the suggestion of G. Hansen, the author began to work on a new design for a gas and liquid interferometer which was based on

physical beam splitting (splitter plate) and provided sufficient brightness if large apertures were used. The interferometer was of the Michelson type, in which the beam splitting is achieved by means of a Kösters prism, as in the case of the meter comparator /19/; the measurement and comparison chambers could thus again be placed directly next to each other. However, the war and post-war conditions prevented the manufacture of this device.

2. Principle of the New Gas and Liquid Interferometer

On the basis of the experience gained in the course of this work, a new interference refractometer has now been developed. This device is also based on the Michelson beam path; however, the beam splitter is no longer a Kösters prism but a combination of two rhombic prisms which can be manufactured more easily and more accurately. In this beam splitter, the path difference in the glass is cancelled by the "end-mirror". As Figure 6 shows, one of the split beams (M) is reflected on the front and the other (V) on the rear surface of the end mirror. The end mirror Sp and the beam splitter T are made from the same batch of glass. The measurement and comparison chambers are situated between the beam splitter and the end mirror. Whilst other devices habitually provide a special end mirror for each of the two beam paths /9/, in this case a single mirror was chosen for both. As a result, the stability of the equipment is particularly high. If the mirror and the beam splitter move in relation to each other, the homologous beams in M and V are always deflected by the same amount and in the same direction, so that the distance between the fringes, once set, remains absolutely unaltered. The interference fringes cannot, therefore, be adjusted by tilting an end mirror. Special devices are required for this purpose. It was decided to use a pair of rotating wedges in the beam path V, compensated by two sliding wedges in beam path M. The sliding wedges make it possible to compensate not only the path difference caused by the pair of rotating wedges, but also any remaining small glass path difference between the end mirror and the beam splitter. In order to prevent possible dislocations between beam splitter and end mirror from giving rise to measurement errors

deriving from changes in path lengths, a fiducial beam path, like in the Haber and Löwe device (Figure 5), is inserted below the measurement and comparison chambers. This fiducial beam path provides the reference point for the interference fringe system of the measuring beam path. Any fringe shifts produced by temperature effects or other disturbances affect the measuring and fiducial beam paths in an identical manner and can thus be easily eliminated. In Figure 6, a measurement chamber and a comparison chamber are outlined at M and V. Chambers of different lengths are available, notably chambers with a length of up to 25 cm for the measurement of gases, and shorter chambers for the measurement of liquids. The chambers for liquids are surrounded by a jacket for temperature control which can be connected to a thermostat.

3. Compensator and Dispersion

The difference Δn in the refractive power of the substances in the measurement and comparison chambers is measured by means of a four-plate compensator, which was proposed in this form by P. Dopp and by R. Torge. Of the four plates, one plate in the measurement and one in comparison beam paths can be rotated on a common axis during measurement; let δ denote the angle of rotation. These two plates have, however, different thicknesses D_1 and D_2 and different powers of refraction N_1 and N_2 and form already at the outset different angles φ_1 and φ_2 with the direction of the light. The two remaining plates are not rotated during measurement; they are identical to the rotating plates and serve mainly to compensate the rotating part in the zero position. They also make it possible, before measurement actually begins, to effect coincidence between the measurement and the fiducial system and to set the measurement system to zero; it order to achieve this, one compensator plate extends into the fiducial beam path. The compensator has one significant property: there is a linear relationship between the angle of rotation and the path difference G caused by the rotation, and the compensator can have different effective dispersions. The path difference G, which is created by or compensated by the four-plate compensator, corresponds to h interference fringes of the

wave-length λ . The path difference is given by:

$$\begin{aligned} G = h \cdot \lambda = 2\,D_1 \,[&\sqrt{N_1^2 - \sin^2(\varphi_1 + \delta)} - \sqrt{N_1^2 - \sin^2\varphi_1} \\ &- \cos(\varphi_1 + \delta) + \cos\varphi_1] \\ - 2\,D_2 \,[&\sqrt{N_2^2 - \sin^2(\varphi_2 + \delta)} - \sqrt{N_2^2 - \sin^2\varphi_2} \\ &- \cos(\varphi_2 + \delta) + \cos\varphi_2]. \end{aligned}$$

If the above expression is expanded in powers of the angle of rotation δ , it is possible, by the appropriate choice of glass types, thicknesses and angles, to cause the quadratic terms to disappear with the cubic terms, and thus obtain very good linearity. In our compensator, the deviations in the measurement range of up to 150 fringes are noticeably smaller than 0.01 interference fringe. In analogy with G. Hanson /11/, we adopt the following definition for the effective dispersion v^* of the compensation equipment:

$$v^* = \frac{G}{\sum_i \frac{\delta G}{\delta N_i} \cdot \Delta N_i} \approx \frac{G}{\Delta G} = \frac{G_e}{G_F - G_C} \qquad \begin{aligned} e &= 5460{,}740\ \text{Å} \\ F &= 4861{,}327\ \text{Å} \\ C &= 6562{,}725\ \text{Å} \end{aligned}$$

The indices e, F and C characterise three wavelengths. If both chambers M and V have an effective length L, and are filled with substances with the refractive powers n_1 and n_2, the path difference G' caused by the chamber fillings is

$$G' = h' \cdot \lambda = 2L(n_1 - n_2)$$

In analogy to v^* , the dispersion $\bar{v}$ of the chamber fillings can be defined as

$$\bar{v} = \frac{G_e}{G_F - G_C} = \frac{(n_1 - n_2)_e}{(n_F - n_C)_1 - (n_F - n_C)_2}$$

When measurement is effected with white light, it is of advantage if the effective dispersion v^* of the compensation equipment coincides as closely as possible with the dispersion $\bar{v}$ of the substances to be measured; in this way, the absence of colour in the zero fringe is retained as the characteristic which distinguishes the zero fringe from the higher order interferences. On the other hand, if the dispersions v^* and $\bar{v}$ are very different, the characteristic of minimum colouring moves from the zero fringe to interference fringes of an increasingly higher order

as the path difference increases /6/, /11/, /12/. This phenomenon causes discontinuities in the calibration curve /14/, whose position can be calculated by means of the formulas indicated by G. Hansen /11/. A description can most easily be given by introducing the following quantity A as a function of the dispersion values v^* and $\bar{v}$:

$$A = \frac{0{,}5 \cdot \nu^*}{\nu^* - \bar{\nu}} \cdot (1 + \bar{\nu} \cdot 0{,}31166)$$

The discontinuities in the calibration curve occur then at those fringe numbers h of the interferometer scale which, in absolute value, correspond to the odd multiples of A, i.e. at $h = /A/, 3/A/, 5/A/, \ldots$ If A is positive (negative), the lack of colour moves towards a larger (smaller) fringe number. The larger /A/, the fewer discontinuities will occur. However, the dispersion values $\bar{v}$ are spread over a wide range. For a complete elimination of discontinuities, it is necessary to use either a variable dispersion compensator or a special compensator for each specific pair of substances. G. Hansen has shown that it is possible with a four-plate compensator to change the effective dispersion within wide limits by combining different glasses. Of course, the requirement $v^* = \bar{v}$ or $A = \infty$ need not be rigorously complied with. As a rule $/A/ \geq 100$ is sufficient since a measurement range of more than 100 fringes is usually not required. Except for a few negative values, the $\bar{v}$ - values of the most frequently measured gases and liquids lie between 20 and 90. Our apparatus was therefore provided with a fixed-dispersion compensator; the value $v^* = 55$ of this standard compensator is selected in such a way that it lies approximately in the middle of the above-mentioned range of $\bar{v}$ values. Hence, the calibration curve has no, or only a few discontinuities for the substances which are most frequently measured. If necessary, it is also possible to use a special compensator with suitable glasses in order to ensure perfect adaptation to a given task, but such a procedure will only be needed in special cases, since the few discontinuities in the calibration curve can easily be determined experimentally by a previous calibration with the substances concerned, using the

method described in /17/ and taken into account when the evaluation is made.

4. Optical Arrangement and Accuracy of Measurement

The most significant parts of the optical layout of the illumination and image-forming beam paths are shown schematically in Figure 7. The light source 1 is a 6-volt/15 watt white-light lamp. A precision line-filter with a narrow band pass for the green mercury line is incorporated in the interferometer in such a way that it can be brought into and taken out of operation, so that observation of the interference in monochromatic light is likewise possible at any time. In order to satisfy all demands which may be placed on the light source, the universal lamp-housing is also fitted to receive other light sources, such as various types of mercury vapour lamps, spectrum lamps of various types, or stronger white-light lamps which might perhaps be desirable for photoelectric measurements. In order to avoid heat problems when very intense light sources are used, high-power heat filters are incorporated; furthermore, the lamp-housing is separated from the interferometer and its connection to the latter has a good thermal insulation. Various types of filters can be used in addition. The light source 1 is projected through the collector 2 onto the aperture stop 4 which lies in the focal plane of the collimating lens 5, so that the beam splitter T and the interference part are penetrated in the parallel beam path. Next, the lens 6 projects an image of the aperture stop in the vicinity of prism 7. Finally, a further image of the aperture stop is obtained at the position of the eye-pupil, the eye-piece 9 being used as exit pupil of the instrument. Near the collector 2 is the radiant-field stop 3, which is adapted to the chamber cross-section and the dimensions of the two interference beam paths. The end mirror Sp (see Figure 6) and the field of vision 8 with the interference fringes are optically conjugate to the radiant-field stop. The axis of rotation of the compensator is denoted by 10. Rigidly attached to it is a long arm, the free end of which carries the transparent measurement scale 11. This scale has equally spaced graduations, because of the linear relationship

between the rotation δ of the compensator on the one hand and the path difference G or the fringe numbers h on the other. The obvious next step was therefore not to use a random graduation, but to calibrate the scale directly in fringe numbers of the green mercury line e = 5450.7 Å in order to eliminate the need for conversion. The part of the scale used for the measurement in progress is illuminated by a beam path not shown here, which corresponds to that of a microscope; after passing through the partly transparent prism 7 the magnified image of this part of the scale is then projected onto the field of view 8; it appears there on a double line which is located between the two interference fringe images produced by the measuring and fiducial beam paths. In this way it is possible to see both interference fringe systems and the measurement value through the same eye-piece. To ensure that the adjustment of the interferences and the read-out of the measurement value do not intrude on each other, each beam path can be screened out with an alternating shutter. The images which appear in turn in the field of vision of the measurement eye-piece are shown side by side in Figure 8. On the left, the two interference fringe systems are shown in coincidence position: the upper image is that of the measurement system and the lower one that of the fiducial system. The considerable distance between the fringe systems is also advantageous for photoelectric control. The two index marks are rigidly linked with each other as described in /16/. The adjustment needed to bring the dark interference fringe into symmetry with the cross-hairs can be performed very precisely. As a rule, adjustments are made only to the measuring system. The fine adjustment of the fiducial system is only performed from time to time if very precise measurements are required and a deviation should be noted. Any correction made to the fiducial system is then automatically transferred to the measuring system. On the right-hand side of Figure 8 one of the graduations of the measurement scale is trapped between the double line of the eye-piece. As shown in the Figure, the fringe number is read off directly, without interpolation, to 100th of a fringe. According to measurements carried out on gases, this value of 100th of the width of the fringe corresponds to the

accuracy of a complete measurement, provided the temperature has been determined with sufficient care. In this way, it is possible to obtain, with the 25 cm chamber in the new interferometer, an accuracy which would have necessitated a 2 m chamber in the earlier model (Figures 4 and 5). In accordance with the formula for G', a refractive power difference $n_1 - n_2$ of 10^{-8} corresponds to the value h' = 0.01. If n_2 is known, n_1 is determined by the measurement to this accuracy. The comparison chamber can also be evacuated, so that absolute values can be measured.

The high-measurement accuracy of the interference refractometer thus leads to the use of correspondingly smaller chambers, where it is easier to effect a precise temperature control. This is important, since the accuracy of a refraction measurement is very frequently limited by the inadequate precision with which the temperature of the measurement array can be controlled. This is also true for the chambers used for liquids, although these are shorter.

5. Construction Details and External Appearance of the Equipment

Figure 9 gives a general view of the interference refractometer. The left-hand side of the apparatus contains the interference beam path with the measurement chambers. The equipment shown in Figure 9 has a gas chamber with an effective length of 25 cm; two of its outlets are visible. During measurement, the cover on top of the chambers remains closed; the thermometers which are closely linked with the chambers can be read off through a window. The right-hand side of the apparatus contains the beam paths for illumination, observation and measurement and all the controls. The measurement eye-piece is denoted by 9, the compensator drive by 12, and the chimney of the lamp-housing at the back of the equipment is denoted by 13. The remaining knobs serve to actuate the interference filter (14), to effect the zero setting of the measuring and fiducial systems (15), and to operate the alternating shutter (16). Figure 10 shows an isolated gas chamber with its

thermometers. Instead of simple hose adapters, valves and fritted glass dust filters have been screwed into the gas inlet and outlet nipples. These parts project from the interferometer (Figure 9), so that there are no hose connections inside the equipment which would need maintenance. It is also possible to replace the gas chambers in the interference refractometer by a temperature vessel with a liquid chamber (Figure 11). The measurement chamber is immersed deeply into the temperature bath. The casing of the temperature vessel is traversed by the temperature coils. Figure 11 shows the four inlet and outlet nipples in the event of connection to a thermostat. Two separate routes are used for the circulation of the heating liquid, so that the circulation in the heating bath and heating jacket can be effected separately or jointly. In this way it is possible to vary the temperature rapidly if necessary, and ensure a constant temperature when measurements are being carried out.

6. Measurement and Automation

The measurement process will be described very briefly, taking gas measurement as an example. After both chamber halves have been rinsed with the comparison gas, the eye-piece and compensator measurement scales are set to zero, and, if necessary, the coincidence setting of the two fringe systems is corrected before actual measurement begins. It is therefore afterwards not necessary to take a zero value into account. After the measurement chamber has been filled with the gas under examination and the temperature and pressure equalized, the zero fringe of the white-light interference in the measurement beam path is again set on the cross-hairs, and, if necessary, this measurement is also repeated for the fiducial beam path. Whilst observations continue to be made through the eye-piece, the alternating shutter is activated, one line of the measurement scale is made to cover the double line of the eye-piece, and the result is read off directly in fringe numbers, as is shown in Figure 8.

In the majority of laboratory experiments, it should be possible to accomplish this simple visual measurement process without difficulty. If, however, examinations have to be carried out continuously as a matter of routine, the use of photoelectric equipment should provide a welcome simplification; a device has therefore been developed in which all interference settings (zero setting, correction, measurement), are made photoelectrically. In addition, the read-out of the measurement values can be digitized, so that this version of the interference refractometer is fully automated. The measurement values can then be read out or printed out in numerical values; if necessary, they can also be fed into a computer, or used for automatic process or production control. A more detailed report on this will be given in due course.

References

1. Th. Young. A Course of Lectures on Natural Philosphy and the Mechanical Arts. Taylor and Walton, London. 1845. Bd.I.S. 359-372. Bd. II Tafel XX and XXX.

2. A. Fresnel. Oeuvres complètes d'Augustin Fresnel. Paris. 1866.

3. F. Arago. Sämtliche Werke. Deutsche Originalausgabe. Leipzig. 1859. S. 257-271.

4. D. Brewster. The Cabinet Cyclopaedia. Treatise on Optics. London. 1831. S. 111.

5. M.J. Jamin. Description d'un nouvel appareil de recherches, fondé sur les interférences. Comptes rendus (Paris) 42, 1856 482-485 and Neuer Interferential-Refractor. Poggendorfs Ann.98. 1856. 356-349.

6. W. Hallwachs. Ann.Phys. Lpz. 47. 1892. 380-398.

7. Lord Rayleigh. Proc. Roy. Soc. London 59. 1896. 198-208.

8. F. Haber. Z. angew. Chem. 19. 1906. 1418 and Z. Elektrochem. 13. 1907. 460.

9. F. Haber and F. Löwe. Angew. Chemie 23. 1910. 1393-1398.

10. F. Löwe. Physik. Zeitschr. 11. 1910. 1047-1051.

11. G. Hansen. Z. Instr. kde 50. 1930. 460-474.

12. E. Karwat. Z. Instr. kde.53. 1933. 12-21 and 70-78.

13. W. Geffcken and A. Kruis. Z. physik. Chemie B 23. 1933. 175-192.

14. W. Kinder. Zeiss-Nachrichten 2. Folge. Heft 7. 1938. 223-233.

15. F. Löwe. Optische Messungen des Chemikers und des Mediziners. 4. Auflage. Dresden and Leipzig. 1943.

16. W. Kinder. Interferometer zu Messzwecken DBP. 1022032.

17. W. Kinder. Zeiss-Werkzeitschrift 4. 1956. 19-24/Nr. 19.

18. W. Nebe. Jenaer Jahrbuch 1958. 2. Teil. 62-101.

19. W. Kinder. IfAG-Mitt. Nr. 58. Deutsche Geodät. Kommission bei der Bayer. Akad. der Wissenschaften. Reihe B. Angewandte Geodäsie - Heft Nr. 95. Teil 1. 1963.

Manuscript received on 12 April 1966.

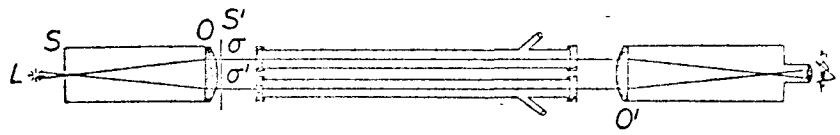

Fig. 1. Diagram of Arago's interferometer.

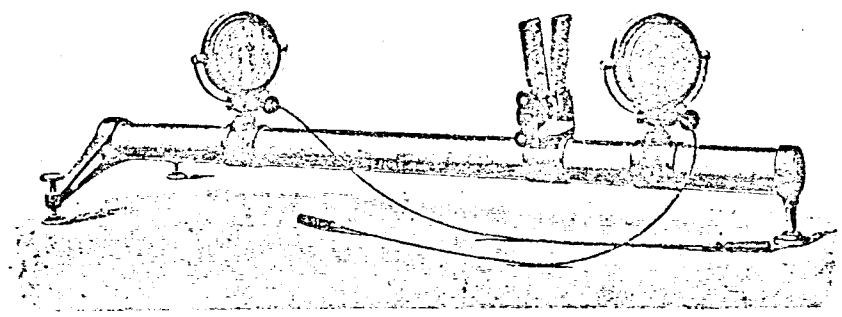

Fig. 2. Jamin interferometer with compensator (Carl Zeiss, c. 1900).

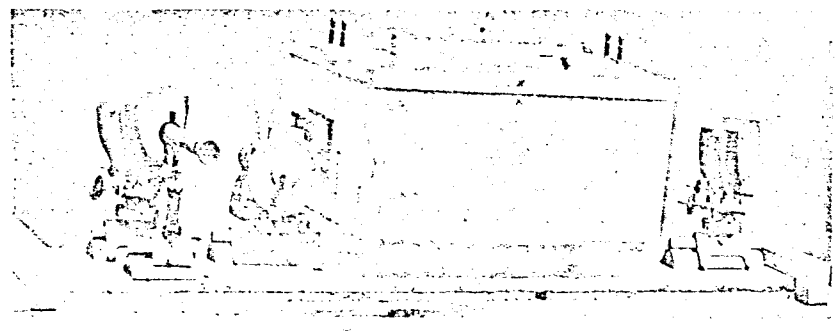

Fig. 3. Carl Zeiss Jamin interferometer, made for F. Huber (c. 1905).

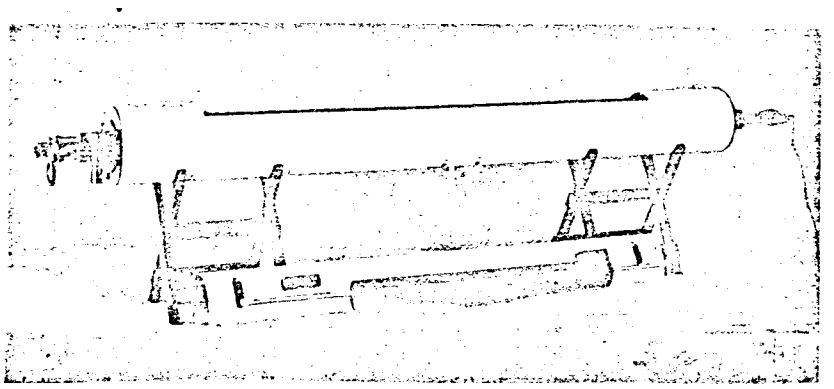

Fig. 4. Laboratory interferometer by Carl Zeiss. Device produced in 1941.

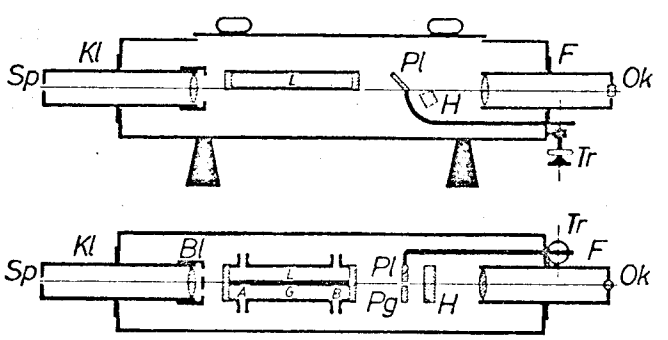

Fig. 5. Optical layout of the laboratory interferometer by Haber and Löwe (Zeiss Journal, 1926).

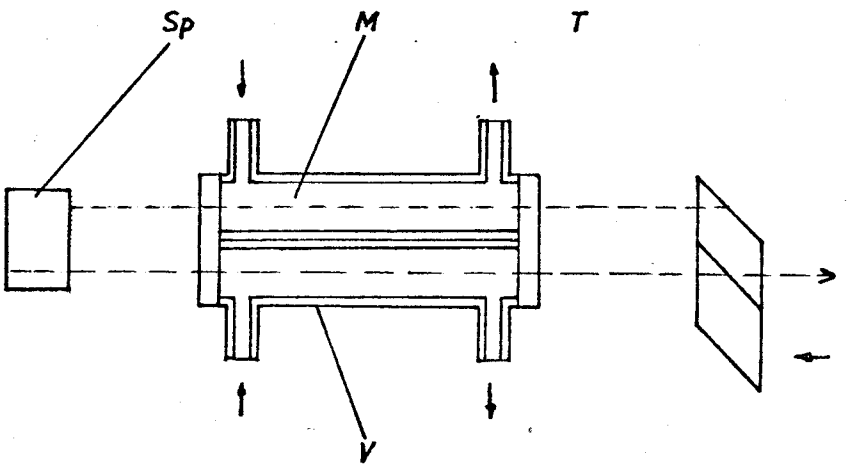

Fig. 6 Diagram of the interference section.

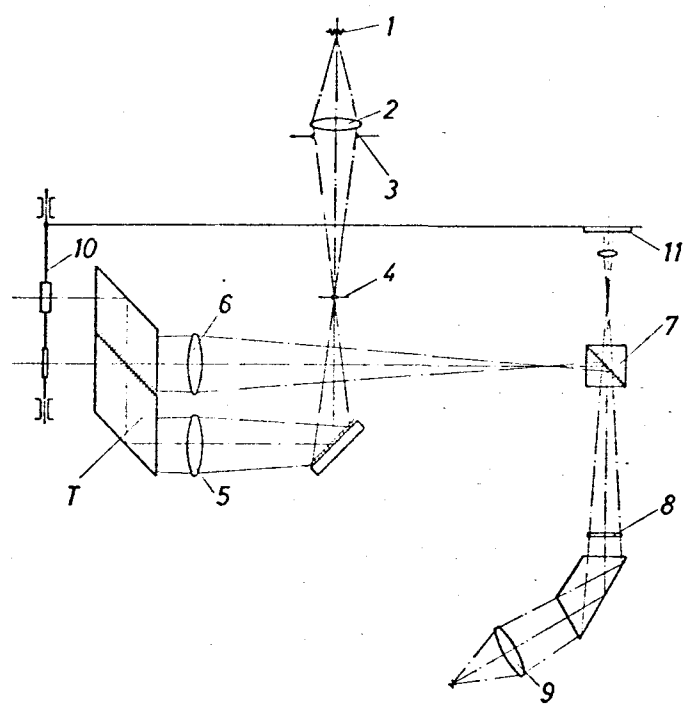

Fig. 7. Illumination and image-forming paths.

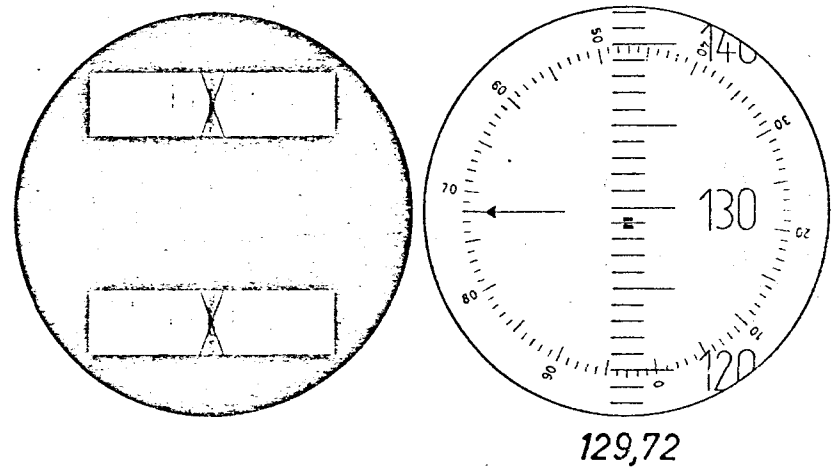

Fig. 8. Field of the measurement eye-piece.

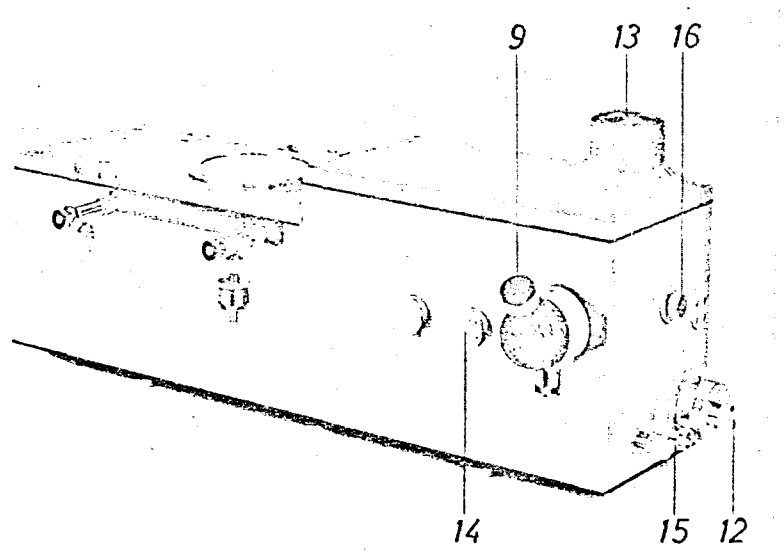

Fig. 9. General view of the new interference refractometer.

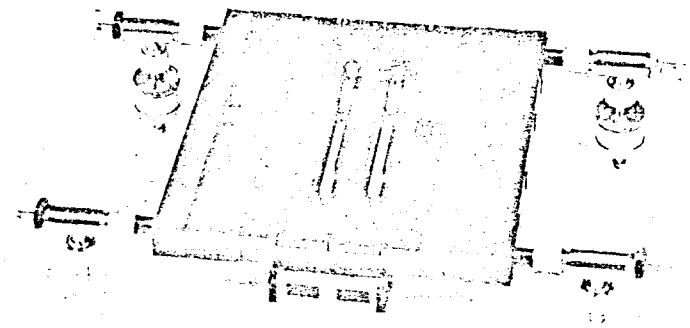

Fig. 10. 25 cm gas chamber.

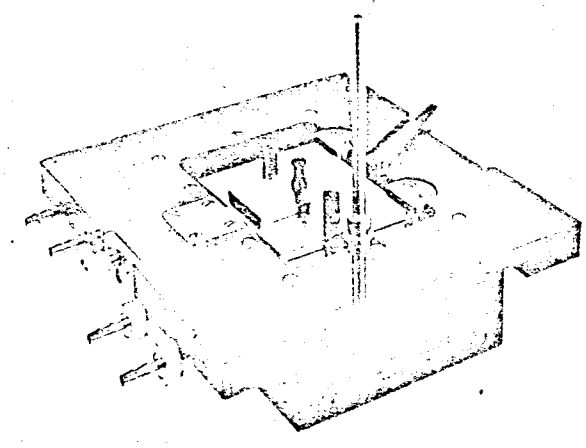

Fig. 11. Temperature vessel and liquid chamber.